Virus Research 277 (2020) 197826

Contents lists available at ScienceDirect

Virus Research

journal homepage: www.elsevier.com/locate/virusres

# Genomic characterization of a novel circovirus from a stranded Longman's beaked whale (*Indopacetus pacificus*)

Nelmarie Landrau-Giovannetti[a], Kuttichantran Subramaniam[a], Melissa Ann Brown[b], Terry Fei Fan Ng[c], David S. Rotstein[d], Kristi West[e,f], Salvatore Frasca Jr.[g], Thomas B. Waltzek[a,*]

[a] Department of Infectious Diseases and Immunology, College of Veterinary Medicine, University of Florida, Gainesville, FL, United States
[b] Molecular Histotechnology Laboratory, College of Veterinary Medicine, University of Florida, Gainesville, FL, United States
[c] College of Veterinary Medicine, University of Georgia, Athens, GA, United States
[d] Marine Mammal Pathology Services, Olney, MD, United States
[e] Hawaii Institute of Marine Biology, University of Hawaii at Manoa, PO Box 1346, Kaneohe, HI, United States
[f] Department of Human Nutrition Food and Animal Science, College of Tropical Agriculture and Human Resources, 1955 East-West Road, University of Hawaii at Manoa Ag Sci 216, Honolulu, HI 96822, United States
[g] Department of Comparative, Diagnostic, and Population Medicine, College of Veterinary Medicine, University of Florida, Gainesville, FL, United States

ARTICLE INFO

*Keywords:*
Longman's beaked whale
Circovirus
*In situ* hybridization assay
Hawaii
Marine mammal
Co-infection

ABSTRACT

Tissues from a juvenile Longman's beaked whale that stranded in Hawaii in 2010 were screened for viruses using a Next-Generation Sequencing (NGS) approach. From the NGS data, the full genome (1,849 bp) of a novel beaked whale circovirus (BWCV) was determined. Two open reading frames (ORF) were annotated, including ORF1 that encodes the capsid gene, ORF2 that encodes the replication-associated gene, and a 9-bp conserved nonamer on the apex of the open loop found in all circoviruses. Independent phylogenetic analyses based on amino acid sequence alignments of the two CV proteins supported the BWCV as a member of the genus *Circovirus,* branching as the sister species to the recently discovered canine circovirus. A sequence identity matrix generated from complete genome alignments revealed the BWCV displays between from 51.1 to 56.7% nucleotide identity to other circoviruses, which is lower than the 80% threshold proposed for species demarcation. Considering the genetic and phylogenetic analyses, we propose the formal species designation of beaked whale circovirus. An endpoint PCR assay targeting the BWCV genome confirmed the presence of the BWCV DNA in every tissue from which DNA was extracted, including spleen, muscle, left ventricle, left adrenal gland, liver, lung, cerebrum, cerebellum, and lymph node. An automated *in situ* hybridization assay utilizing RNAscope® technology and targeting the replication-associated gene resulted in labeling of individual cells morphologically resembling mononuclear leukocytes and cells of blood vessels in diaphragm, liver, lymph nodes, lung, pericardium, oral mucosa and tongue, adrenal gland, testis, aorta, intestine, stomach and heart. The clinical or pathologic significance of BWCV is undetermined, as are its host range, prevalence, and pathogenicity in cetaceans of Hawaiian waters and elsewhere.

## 1. Introduction

Members of the family *Circoviridae* are small non-enveloped viruses with icosahedral nucleocapsids of approximately 17 nm in diameter that enclose a single-stranded (ss) circular DNA (ssDNA) genome ranging in size from 1.7 to 2.3 kilobases (Herbst and Willems, 2017). The ambisense genome contains two open reading frames (ORFs) that encode the capsid and replication-associated proteins (Biagini et al., 2012). The intergenic region between these genes contains a conserved nonamer at the apex of a stem-loop motif where replication of the ssDNA genome is initiated and then completed by rolling circle mechanism (Biagini et al., 2012). According to a recent taxonomic revision of the family *Circoviridae*, the family is divided into the genera *Circovirus* and *Cyclovirus* (Breitbart et al., 2017). The genus *Circovirus* currently includes 39 recognized species from ticks (2), fish (2), birds (12), bats (11), pigs (3), dog (1), rodents (6), human (1), and chimpanzee (1) (Breitbart et al., 2017). The genus *Cyclovirus* currently includes 48 recognized species from invertebrates (9), birds (2), bats (16), humans

* Corresponding author at: Department of Infectious Diseases and Immunology, College of Veterinary Medicine, University of Florida, 2187 Mowry Road, 32611 Gainesville, FL, United States.
*E-mail address:* tbwaltzek@ufl.edu (T.B. Waltzek).

https://doi.org/10.1016/j.virusres.2019.197826
Received 31 July 2019; Received in revised form 26 November 2019; Accepted 26 November 2019
Available online 29 November 2019
0168-1702/ 

(12), and other mammals (9) (Breitbart et al., 2017). However, the exact host range of cycloviruseses is not known as many have been discovered in the feces or gut samples as opposed to being detected in blood or tissue samples (Breitbart et al., 2017; Li et al., 2010).

The genus *Circovirus* includes agents responsible for diseases of veterinary significance such as *Porcine circovirus 2* (PCV2). *Porcine circovirus 1* (PCV1) was first identified in 1974 in a persistently infected permanent pig kidney cell line and is considered nonpathogenic to pigs (Tischer et al., 1974). *Porcine circovirus 2* was discovered in 1997 from Canadian pigs pigs displaying post-weaning multisystemic wasting syndrome (PMWS) (Nayar et al., 1997). PCV2 causes various disease syndromes in pigs, known collectively as porcine circovirus-associated disease (PCVAD), including: PMWS, porcine dermatitis and nephropathy syndrome (PDNS), proliferative and necrotizing pneumonia (PNP), reproductive failure, and enteritis. Another manifestation of PCVAD is the development of subclinical infections (i.e., PCV2-SI), which is linked with growth retardation without overt clinical signs (Segalés, 2012). PCVAD is one of the most economically important disease syndromes in the swine industry and occurs most commonly in piglets of 5–18 weeks of age (Segalés et al., 2013). The most common microscopic lesions observed with PCVAD include mild to severe lymphocyte depletion with an accompanying granulomatous inflammation within lymphoid tissues (Segalés, 2012). Thus, it is believed that PCV2 is immunosuppressive, which predisposes infected pigs to secondary infections. Other microscopic lesions include necrotizing bronchiolitis, interstitial nephritis, non-suppurative to necrotizing or fibrosing myocarditis of fetuses, and hepatic congestion in fetuses (Segalés, 2012). PCV2 infected cells may display basophilic botryoid (grape-like) inclusion bodies within the cytoplasm. *Porcine circovirus 3* (PCV3) was recently detected in three pigs with cardiac pathology and multi-systemic inflammation from Missouri (Phan et al., 2016). In addition, *in situ* hybridization (ISH) detected PCV-3 nucleic acids in heart lesions, corroborating virus infection and identifying PCV-3 as a potential contributing cause of clinical disease in pigs (Phan et al., 2016). More recently, PCV3 was identified in pigs on a farm in North Carolina displaying PDNS, reproductive failure, and multi-systemic inflammation (Kwon et al., 2017; Palinski et al., 2017).

Lorincz and colleagues (2011) characterized the first circovirus in an aquatic vertebrate, diseased barbel fry (*Barbus barbus*). Their metagenomic analyses of the moribund fish recovered two complete genomes, barbel circovirus 1 (BaCV1) and barbel circovirus 2 (BaCV2), but linkage of these viruses to disease was not established (Lorincz et al., 2011). Another fish circovirus, the *European catfish circovirus* (EcatfishCV), was detected in spawning sheetfish (*Silurus glanis*) experiencing high mortality in Lake Balaton, Hungary in 2011 (Lorincz et al., 2012). As circoviruses generally have been considered to be immune-suppressive, it was speculated that the EcatfishCV played a role in the observed mortality that occurred during the stress of spawning (Lorincz et al., 2012).

A number of studies have sought to understand the mechanism by which circoviruses induce host immunosuppression. Shibahara et al. (2000) reported PCV2 induces apoptosis in B lymphocytes, which leads to B lymphocyte depletion and therefore suppression of humoral immunity. Abadie et al. (2001) demonstrated a significantly higher percentage of apoptotic lymphocytes in the bursa of Fabricius of birds infected with *Pigeon circovirus* (PiCV) than in uninfected birds.

*In situ* hybridization is a molecular method used to localize specific nucleic acid sequences, DNA or RNA, within tissue sections. Older, conventional, ISH methods have a high degree of technical complexity, but low sensitivity and specificity; RNAscope® technology, on the other hand, is an advance in RNA ISH technology that relies on a proprietary probe design to amplify target-specific signals and to reduce background signal from non-specific hybridization (Wang et al., 2012). A study done by Smyth et al. (2001) found a higher detection (89%) of PiCV using conventional ISH technology compared to their histological examination (66%). It also showed that PiCV was widespread in many tissues of infected birds including liver, kidney, trachea, lung, brain, crop, intestine, spleen, bone marrow, and heart. Choi and Chae (1999) used conventional ISH to detect PCV in formalin-fixed paraffin-embedded tissues from 10 weaned pigs with naturally occurring PMWS. There was labelling for PCV in the lymph nodes, in macrophages of the liver, spleen, Peyer's patches, lung and tonsil, in hepatocytes and in renal tubular epithelial cells (Choi and Chae, 1999). In recent years, ISH has been used to detect circoviruses, including porcine circoviruses 1–3 with the improvement of its technology. Positive staining of PCV3 has been detected in lymphocytes infiltrating the alveolar spaces of the lungs, in macrophages in the alveolar wall, and in histiocytes of the lymph node follicles (Kedkovid et al., 2018; Kim et al., 2018).

In 2010, a juvenile male Longman's beaked whale (*Indopacetus pacificus*) stranded in Maui, Hawaii. Histopathological findings included lymphoplasmacytic periglomerulitis, mild lymphoid depletion, encephalitis, pulmonary edema, thyroid gland atrophy, and bilateral hypertrophy of the adrenal cortex (West et al., 2013). Diagnostic testing using conventional PCR assays detected a novel cetacean morbillivirus and a novel alphaherpesvirus (West et al., 2013). Herein, we report the genomic characterization of a novel circovirus also detected in the tissues of this Longman's beaked whale using a high-throughput sequencing approach, followed by detection of this novel circovirus in tissues by ISH using RNAscope® technology.

## 2. Materials and methods

### 2.1. Samples and genome sequencing

Tissue samples of spleen, muscle, left ventricle, mesenteric lymph node, scapular lymph node, mediastinal lymph node, left adrenal, liver, lung, cerebrum, and cerebellum from a juvenile Longman's beaked whale that stranded in Hawaii (West et al., 2013) were sent frozen on dry ice to the Wildlife and Aquatic Veterinary Disease Laboratory (Gainesville, FL). DNA from lung was extracted using a Qiagen DNeasy Kit (Qiagen, Valencia, CA) following the manufacturer's instructions. A DNA library was prepared by using an Illumina Nextera XT DNA Library Preparation Kit and sequenced by using a 600-cycle V3 Kit on an Illumina MiSeq sequencer (Illumina, San Diego, CA). The paired-end reads were quality trimmed and assembled *de novo* in CLC Genomic Workbench V7 using default settings. BLASTX analysis of the assembled contigs was conducted against the National Center for Biotechnology Information (NCBI) GenBank non-redundant (nr) protein sequence database. A 1,434 bp contig was identified with highest amino acid (aa) identity (91/174; 52%) to a replication-associated protein of canine circovirus (GenBank accession no. AML03152) previously sequenced from the mesenteric lymph node of a dog (*Canis lupus familiaris*). Conventional and inverse PCRs, with primers designed from the known replication-associated gene sequence (Table 1), were implemented to amplify the complete genome sequence of the beaked whale circovirus (BWCV). The Sanger sequence reads were then assembled into a single contiguous sequence and open reading frames (ORFs) were predicted using CLC Genomic Workbench V7. Gene functions were determined based on BLASTP searches against the NCBI GenBank nr protein sequence database.

**Table 1**
Primers used to amplify the complete genome of the beaked whale circovirus (BWCV) and screen Longman's beaked whale tissue samples for BWCV.

| Primer name | Sequence | Comments |
|---|---|---|
| BWCVInv-F1 | AGACTCTCCTTTCTCTCGGC | Amplification of BWCV |
| BWCVInv-R1 | CGGCATCATCGGGGATTTTC | |
| BWCVConv-F2 | CCCGACAGAAGCAGATGAAG | |
| BWCVConv-R2 | TTTAGACTTGCCCACCCCAG | |
| BWCV-F | CTTCAGATTCCCCGTCAAGA | Tissue screening |
| BWCV-R | GTCTCCCCACAATGGTTCAC | |

**Table 2**
Circoviruses used in the phylogenetic and genetic analyses (adapted from Rosario et al., 2017).

| Species name | Abbreviation | Accession # |
|---|---|---|
| Barbel circovirus | BarCV | GU799606 |
| Bat associated circovirus 1 | BatACV-1 | JX863737 |
| Bat associated circovirus 2 | BataCV-2 | KC339249 |
| Bat associated circovirus 3 | BatACV-3 | JQ814849 |
| Bat associated circovirus 4 | BatACV-4 | KT783484 |
| Bat associated circovirus 5 | BatACV-5 | KJ641727 |
| Bat associated circovirus 6 | BataCV-6 | KJ641724 |
| Bat associated circovirus 7 | BatACV-7 | KJ641723 |
| Bat associated circovirus 8 | BatACV-8 | KJ641711 |
| Bat associated circovirus 10 | BatACV-10 | KX756986 |
| Bat associated circovirus 11 | BatACV-11 | KX756996 |
| Beak and feather disease virus | BFDV | AB277746 |
| Canary circovirus | CaCV | AJ301633 |
| Canine circovirus | CanineCV | JQ821392 |
| Chimpanzee associated circovirus 1 | ChimpACV-1 | GQ404851 |
| Duck circovirus | DuCV | AY228555 |
| European catfish circovirus | EcatfishCV | JQ011377 |
| Finch circovirus | FiCV | DQ845075 |
| Goose circovirus | GoCV | AF418552 |
| Gull circovirus | GuCV | DQ845074 |
| Human associated circovirus 1 | HuACV | GQ404856 |
| Mink circovirus | MiCV | KJ020099 |
| Pigeon circovirus | PiCV | AF252610 |
| Porcine circovirus 1 | PCV1 | AF012107 |
| Porcine circovirus 2 | PCV2 | AF027217 |
| Porcine circovirus 3 | PCV3 | KT869077 |
| Raven circovirus | RaCV | DQ146997 |
| Starling circovirus | StCV | DQ172906 |
| Swan circovirus | SwCV | EU056309 |
| Zebra finch circovirus | ZfiCV | KP793918 |
| Tick associated circovirus 2 | TickACV-2 | KX987146 |
| Beaked whale circovirus | BWCV | MN103538 |

### 2.2. Phylogenetic and genetic analyses

The phylogenetic analyses were performed on the full-length predicted aa sequences of the replication-associated and capsid proteins for 32 circoviruses, including BWCV (Table 2). The aa sequences were aligned for each gene in MAFFT 7 using default parameters (Katoh and Standley, 2013). The final data sets contained 379 and 415 aa characters (including gaps) for the replication-associated and capsid genes, respectively. Maximum Likelihood (ML) phylogenetic analyses were performed in IQ-TREE (Nguyen et al., 2014) with the Bayesian information criterion to determine the best model fit and 1000 non-parametric bootstraps to test the robustness of the clades (Nguyen et al., 2014). The phylogenetic trees were then edited using FigTree v1.4.2 (Rambaut, 2014). For the genetic analysis, complete genome sequence of the BWCV was compared to 31 circoviruses using the Sequence Demarcation Tool v1.2 (Muhire et al., 2014) with the MAFFT 7 alignment option implemented (Table 2).

### 2.3. PCR detection of BWCV in Longman's beaked whale tissues

A primer pair specific to BWCV (Table 1) was designed using the Primer3 program (Rozen and Skaletsky, 2000). In a retrospective assay, conventional PCR testing was performed on all 11 available frozen tissues (i.e., spleen, muscle, left ventricle, mesenteric lymph node, left adrenal, liver, lung, cerebrum, cerebellum, scapular lymph node, mediastinal lymph node) to determine the distribution of the BWCV in tissues of the Longman's beaked whale. The 30 µl BWCV PCR cocktail consisted of 0.15 µl of Platinum *Taq* DNA Polymerase (Invitrogen, Waltham, MA), 3.0 µl of 10 × PCR Buffer, 1.2 µl of 50 mM $MgCl_2$, 0.6 µl of 10 mM dNTPs, 1.5 µl of 20 µM forward and reverse primers, 17.55 µl of molecular grade water, and 4.5 µl of DNA template. The following thermal cycling conditions were used for the BWCV conventional PCR assay: one cycle of 94 °C for 5 min for initial denaturation, followed by 40 amplification cycles of 94 °C for 30 s for denaturation, 56 °C for 30 s for annealing, 72 °C for 30 s for elongation, and a final elongation cycle of 72 °C for 5 min. PCR products were then subjected to electrophoresis in a 1% agarose gel stained with ethidium bromide. Fragments of the expected size (400 bp) were purified using a QIAquick PCR Purification Kit. The concentration of purified DNA was quantified fluorometrically using a Qubit® 3.0 Fluorometer and dsDNA BR Assay Kit. Purified DNA was sequenced in both directions on an ABI 3130 Genetic Analyzer (Applied Biosystems, Foster City, CA).

### 2.4. In situ hybridization (ISH)

Archived paraffin blocks of formalin-fixed tissues collected at necropsy (West et al., 2013) were used in an automated *in situ hybridization* (ISH) assay to detect DNA of BWCV. Chromogenic ISH was performed on a Leica BOND RX Fully Automated Research Stainer (Leica Biosystems, Buffalo Grove, IL) using RNAscope® technology (Wang et al., 2012) adapted for the Leica Systems (LS) automated staining platform (Anderson et al., 2016). Probes were designed by Advanced Cell Diagnostics (Newark, California) and prepared for use on the LS platform; probes to the following genes were used: dihydrodipicolinate reductase (*dapB*) [catalog # 312038]; Longman's beaked whale (*Indopacetus pacificus*) cytochrome *B* (*LBW cytoB*) [catalog # 809855]; Longman's beaked whale circovirus replication-associated gene (*BWCV rag*) [catalog # 554198]. Blocks of formalin-fixed paraffin-embedded tissues were sectioned at 4 µm and mounted on

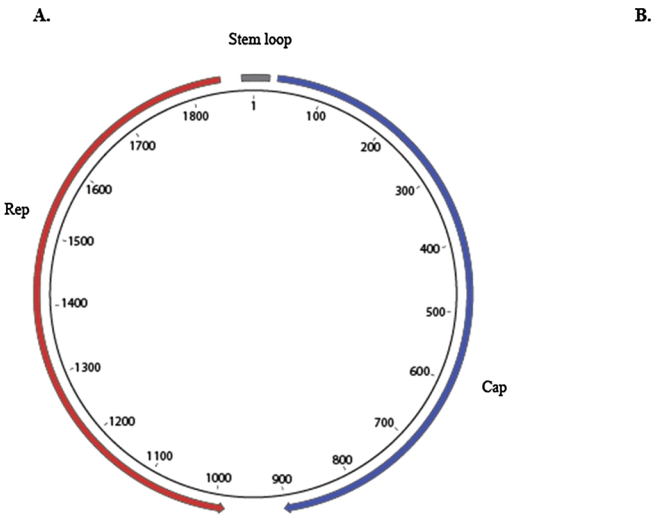


**Fig. 1.** Genome schematics of the beaked whale circovirus (BWCV). A) Two open reading frames (ORFs) were annotated including the capsid protein (Cap) and the replication-associated protein (Rep). B) The stem-loop motif of the BWCV consist of palindromic 15 bp stem and a 11 bp open loop that includes a 9 bp long conserved nonamer (5′-TAGTATTAC-3′) highlighted in yellow.

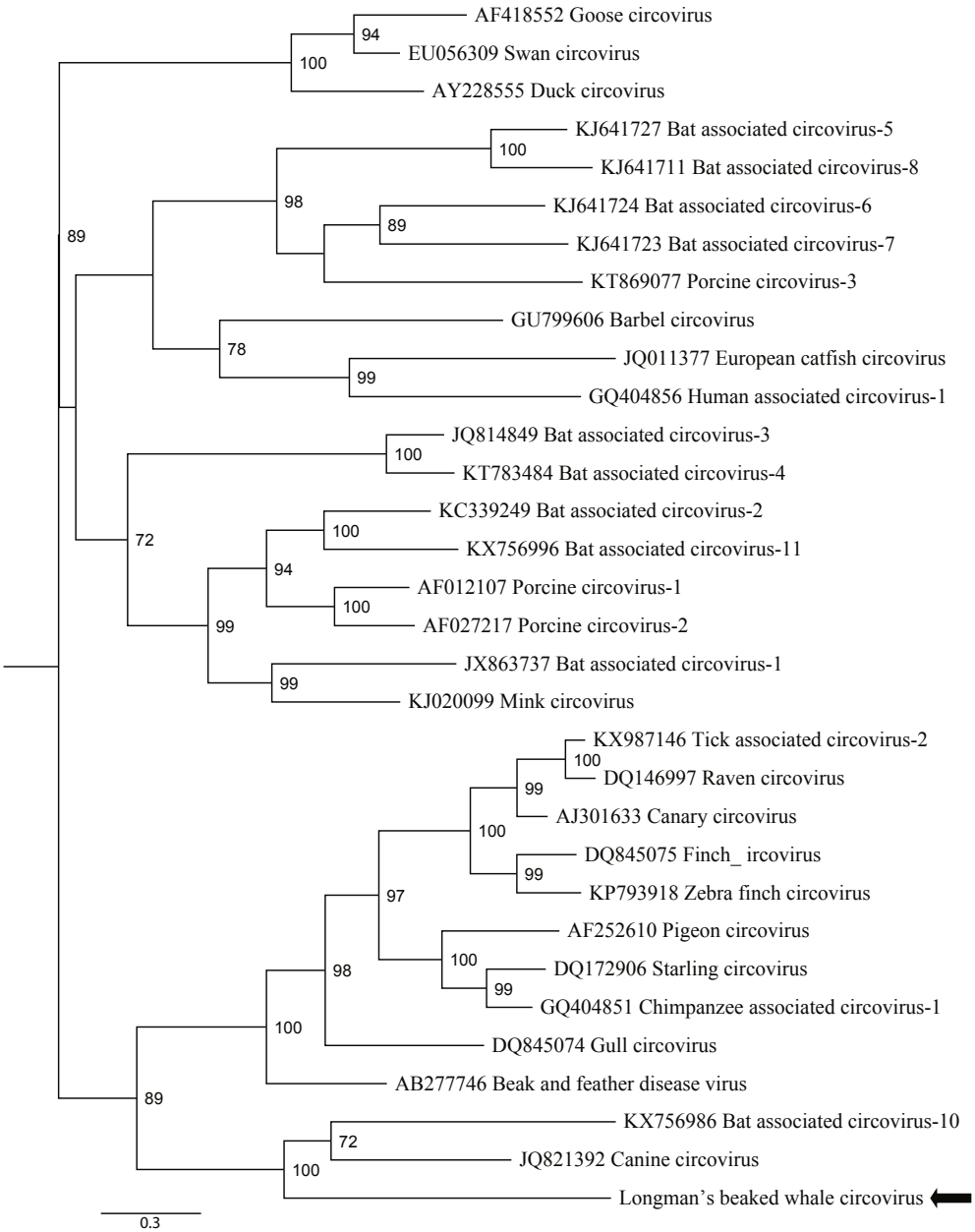


**Fig. 2.** Phylogram depicting the relationship of the beaked whale circovirus (black arrow) from Longman's beaked whale (*Indopacetus pacificus*) to representatives of the genus *Circovirus* based on their aligned capsid amino acid sequences (415 characters including gaps). Bootstrap values of > 70% were indicated at the nodes and the branch lengths represent the number of inferred substitutions as indicated by the scale.

Fisherbrand SuperFrost Plus glass slides (Fisher Scientific, Pittsburgh, PA) for use in a single-plex automated RNAscope® assay with slight modifications to the method of Anderson et al. (2016). The assay was performed on the Leica BOND RX stainer and consisted of four steps, i.e. pretreatment, hybridization, signal amplification, and detection. Pretreatment was carried out by sequential deparaffinization, target retrieval (15 min incubation at 95 °C using Leica Epitope Retrieval Buffer 2), protease digestion (20 min at 40 °C), and endogenous enzyme block. This was followed by target probe hybridization (120 min at 42 °C). Signal amplification was performed through a series of reactions, i.e. RNAscope signal amplification (Wang et al., 2012), that culminated in fast red chromogenic development, and was followed by hematoxylin staining.

The following tissues were subjected to histopathological examination and RNAscope® ISH: diaphragm, liver, five lymph nodes (not specified as to anatomic location), lung, pericardium, oral mucosa and tongue, adrenal gland, testis, aorta, intestine, stomach, spleen, heart, and skeletal muscle. Three sections from each paraffin block were tested in an experimental design wherein one section received the *dapB* (negative control) probe, a second section received the *LBW cytoB* (internal positive control) probe, and a third section received the *BWCV rag* (test) probe. Separate histologic sections at 4 µm were prepared from each paraffin tissue block, mounted on glass slides, and stained with hematoxylin and eosin for comparison. The resultant histologic sections were interpreted using an Olympus BX53 light microscope (Olympus, Center Valley, PA).

## 3. Results

### 3.1. Genomic sequence annotation

The complete circular BWCV genome was determined to be 1889 bp

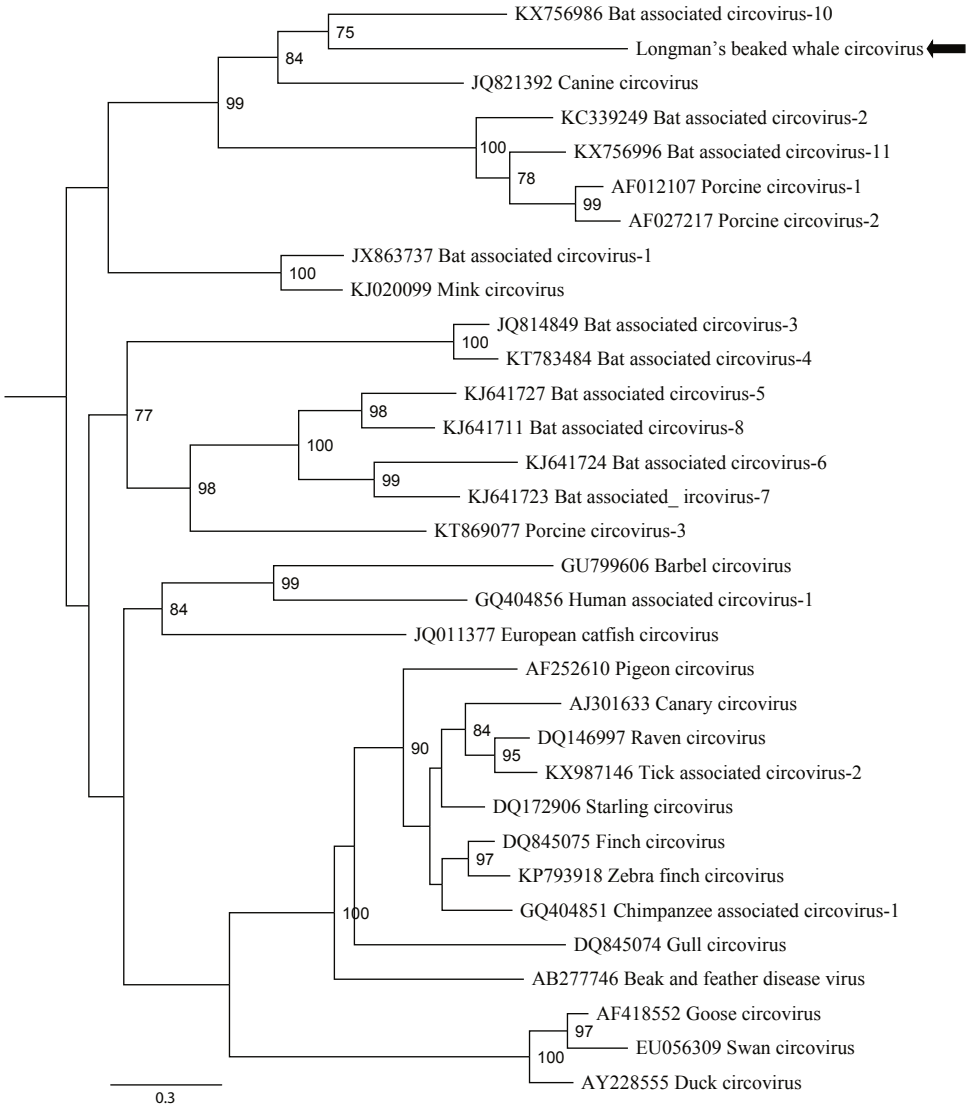


**Fig. 3.** Phylogram depicting the relationship of the novel beaked whale circovirus (black arrow) from Longman's beaked whale (*Indopacetus pacificus*) to representatives of the genus *Circovirus* based on their aligned replication-associated amino acid sequences (379 characters including gaps). Bootstrap values of > 70% were indicated at the nodes and the branch lengths represent the number of inferred substitutions as indicated by the scale.

with a G + C content of 46.5%. Two ORFs were identified, on complementary strands in opposite orientation, which encode the capsid and replication-associated proteins (Fig. 1A). The BWCV contains a stem-loop motif between the intergenic region of the two ORFs which consists of palindromic 15 bp stem, a 11 bp open loop for the initiation of rolling-circle replication, and a 9 bp conserved nonamer (5′-TAGT ATTAC-3′) on the apex of the open loop (Fig. 1B). The replication-associated protein contains 3 rolling circle replication motifs at the N-terminus including, motif I [FTVNN; aa 10–14], motif II [PHLQG; aa 45–49], and motif III [YCSK; aa 84–87]. The superfamily 3 helicase motifs located at the C-terminus of the BWCV replication-associated protein displayed a Walker-A motif [GPPGVGKS; aa 163–170], a Walker-B motif [IIDDF; aa 200–204], and motif C [ITSN; aa 240–243]. The N-terminus of BWCV capsid protein contains a 41-aa-long arginine (R) rich stretch (RRYRRHRPYFRRRRRYHGYRKRFNRRRRFRKPRLFHF-RFER) starting at residue 2. The genome sequence of the BWCV has been deposited under the NCBI GenBank accession no. MN103538.

### 3.2. Phylogenetic and genetic analyses

The ML analyses based on the aligned aa sequences of replication-associated and capsid genes, using the best fit models LG + I+G4 and PMB + I+G4, respectively, produced well-supported trees with the BWCV grouping most closely to the bat associated circovirus 10 and canine circovirus isolate 214 (Figs. 2 and 3; GenBank accession nos. KX756986 and JQ821392, respectively). The nucleotide identity ranged from 51.1 to 56.7% to other circoviruses and the highest aa identity was observed to the bat associated circovirus 2 isolate XOR7 (Fig. 4; GenBank accession no. KC339249).

### 3.3. Detection of BWCV in Longman's beaked whale tissues

A single band of 400 bp was observed for all 11 frozen tissues tested. The resulting edited Sanger sequences were identical to the BWCV genome determined through NGS.

### 3.4. In situ hybridization (ISH)

Histologic sections of tissues that were positive for BWCV by conventional PCR and had demonstrated cellular labeling with the *LBW cytoB* probe displayed labeling of some cells after application of the *BWCV rag* probe. The most intense labeling was seen in lymph nodes,

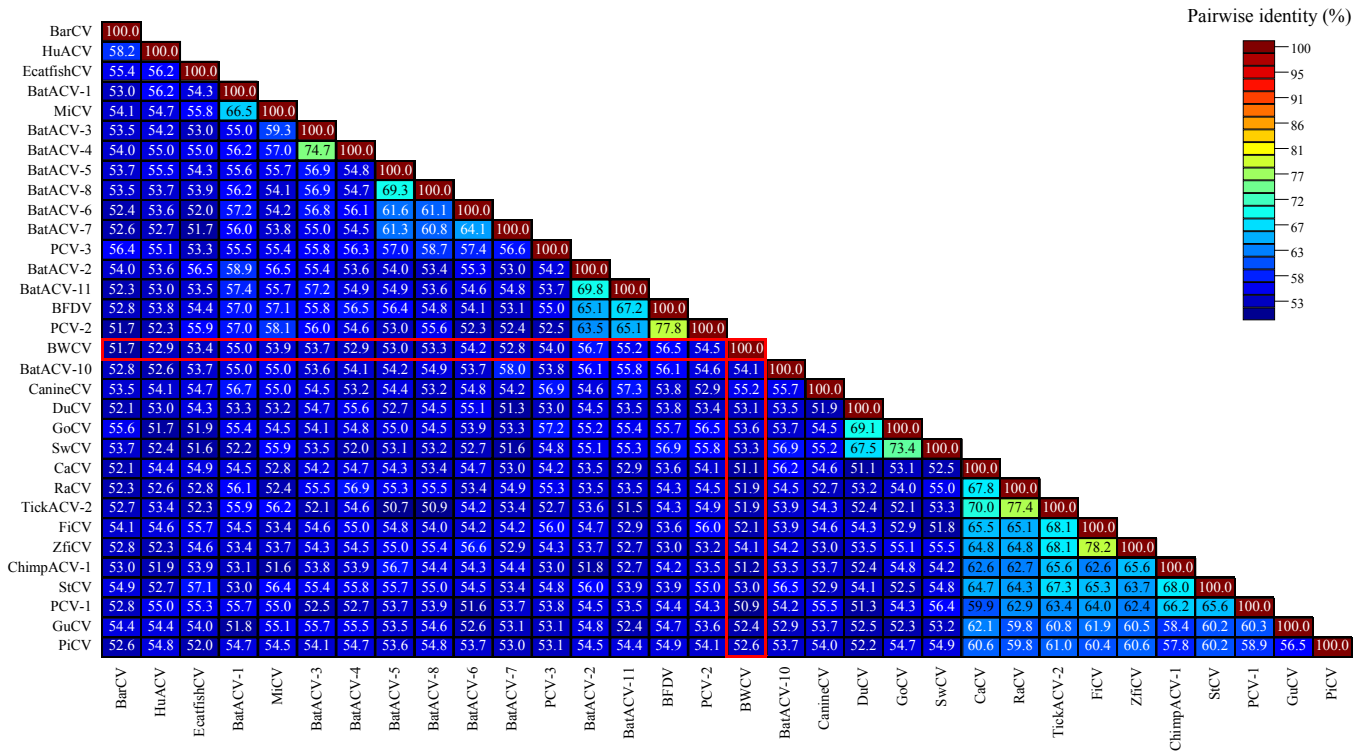


**Fig. 4.** Genetic comparison of the full genome of the novel BWCV from Longman's beaked whale (*Indopacetus pacificus*) to 31 accepted type species in the genus *Circovirus*. Values are expressed as a percentage of nucleotide identity. See Table 2 for circovirus abbreviations.

where high numbers of cells that appeared morphologically to be mononuclear cells, i.e. lymphocytes and macrophages, were labeled by the *BWCV rag* probe (Fig. 5A, B, C). There was labeling of cells that appeared morphologically to be mononuclear leukocytes in the submucosa of the oral mucosa and in the blood vessels of the tongue and capsule of the adrenal gland, and in the lung, where occasional cells along the alveolar walls were labeled (Fig. 5D, E, F). There was labeling of cells that appeared morphologically to be endothelial cells and vascular smooth muscle cells in blood vessels of the examined tissues (Fig. 5G, H, I), bronchial and bronchiolar epithelium, and occasionally in myocardial fibers and gastric glandular epithelium. BWCV nucleic acid was detected in the cells of the zona glomerulosa, hepatocytes, biliary epithelium, and the spermatogenetic epithelium of seminiferous tubules. No reactivity was observed when the *dapB* (negative control) probe was applied to tissue sections of diaphragm, liver, lymph node, lung, pericardium, oral mucosa and tongue, adrenal gland, testis, aorta, intestine, stomach, spleen, heart, and skeletal muscle from the Longman's beaked whale. Host cells in histologic sections of all tissues except spleen and skeletal muscle were labeled by the *LBW cytoB* (internal positive control) probe. Histologic sections of spleen and skeletal muscle were not interpreted further because of the absence of labeling by the internal control probe, which may have been a result of the marked autolysis of those tissues.

## 4. Discussion

The current study provides the first complete genome sequence of a circovirus from a marine mammal, i.e. a Longman's beaked whale. The presence of circoviral nucleic acid in tissues of this Longman's beaked whale was verified by conventional PCR and ISH. The circovirus from this Longman's beaked whale, i.e. BWCV, displayed a typical circovirus genome organization including two proteins (i.e., replication-associated and capsid) and a conserved nonamer (5′-TAGTATTAC-3′) within a stem-loop motif. The BWCV replication-associated protein, containing rolling cycle replication motifs at the N-terminus and superfamily 3 helicase motifs at the C-terminus, mediates the initiation and termination of rolling cycle replication (Ilyina and Koonin, 1992). The BWCV capsid protein displayed an arginine (*R*)-rich N-terminus, which is believed to involve DNA binding and nuclear localization (Sarker et al., 2016).

A methionine (ATG) start codon was not identified for the BWCV capsid protein, and we postulate the use of alternative start codon (GTT; valine) at nucleotide position 1843 in the BWCV genome. Future transcriptomic analyses will be needed to verify the start codon used by BWCV. The use of alternative start codons is commonplace in avian circoviruses (Mankertz et al., 2000; Phenix et al., 2001; Stewart et al., 2006; Todd et al., 2001, 2007). *Porcine circovirus 3* also utilizes an alternative start codon (valine) (Palinski et al., 2017). Although the significance of the usage of an alternative start codon in circoviruses remains to be determined, in eukaryotes and RNA viruses they act as a regulatory mechanism for proteins with key cellular functions (Kearse and Wilusz, 2017) and translation of multiple proteins from alternative reading frames (Firth and Brierley, 2012), respectively.

The BWCV genome sequence reported herein permitted phylogenetic and genetic analyses that support its inclusion as a novel species within the family *Circoviridae*. Phylogenetic analyses based on aa sequences of replication-associated and capsid genes revealed the BWCV branches most closely to bat associated circovirus 10 and canine circovirus isolate 214 (GenBank accession nos. KX756986 and JQ821392, respectively). One criterion for the species demarcation of circoviruses is the genome-wide pairwise nucleotide identity of < 80% represent circoviruses from different species and > 80% represent different strains within a species (Rosario et al., 2017). The genome-wide pairwise identity of BWCV as compared to 31 other circoviruses revealed highest nucleotide identity of 56.7% identity with the bat associated circovirus 2. Given the unique phylogenetic position and sequence divergence of the BWCV, we propose the formal species designation of beaked whale circovirus (BWCV) to be considered for approval by the International Committee on Taxonomy of Viruses.

The clinical significance and pathogenicity of BWCV is unknown,

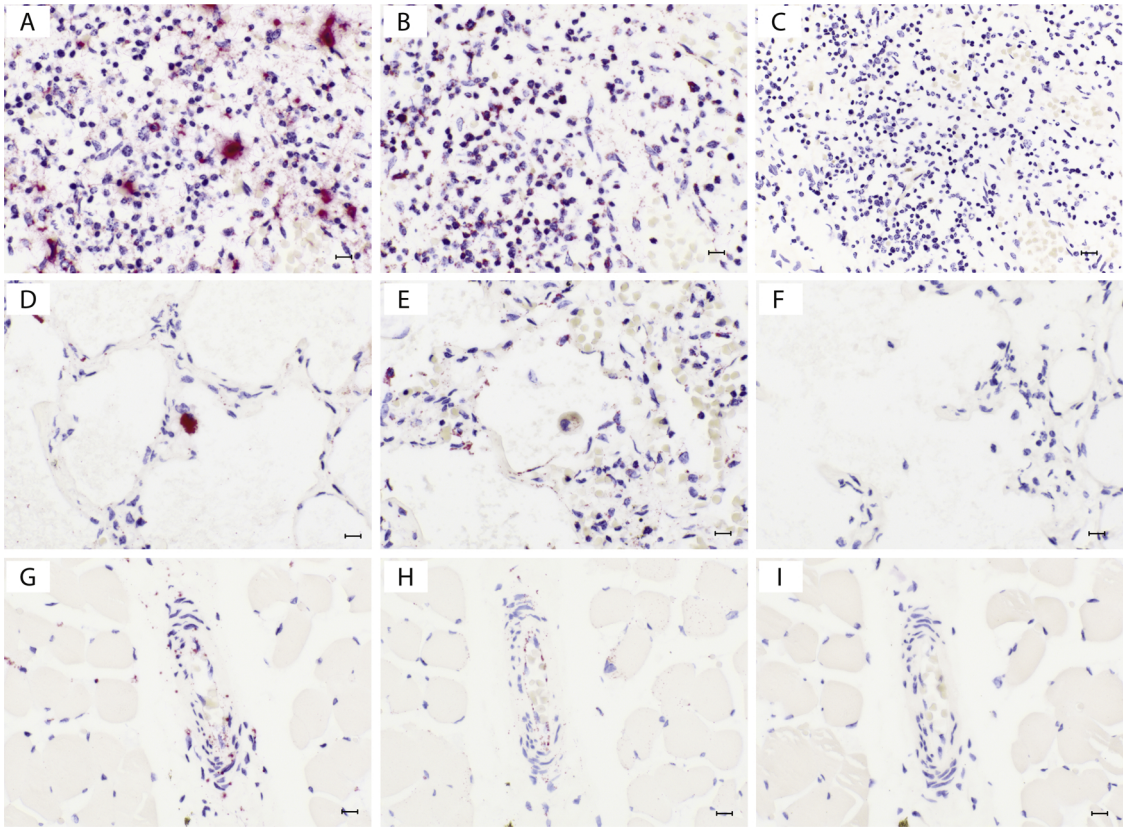


**Fig. 5.** RNAscope® *in situ* hybridization (ISH) results from Longman's beaked whale (LBW) tissues. A) Lymph node (LN) processed with the *BWCV rag* probe: ISH indicates circovirus nucleic acid labeling (red) within cells resembling mononuclear cells; B) LN processed with the *LBW cytoB* positive control probe: labeling (red) is apparent in cells resembling mononuclear cells; C) LN processed with the *LBW cytoB* negative control probe: no labeling (red) is apparent; D) Lung processed with the *BWCV rag* probe: ISH demonstrates circovirus nucleic acid labeling (red) within a cell along the alveolar wall; E) Lung processed with the *LBW cytoB* positive control probe: red labeling is located in the cytoplasm of a cell resembling an alveolar macrophage and in cells along the alveolar wall; F) Lung processed with the *dapB* negative control probe: no labeling (red) is apparent; G) Diaphragm processed with the *BWCV rag* probe: ISH indicates circovirus nucleic acid labeling (punctate red dots) in cells resembling endothelial and smooth muscle cells of the blood vessel; H) Diaphragm processed with the *LBW cytoB* positive control probe: labeling, represented by punctate red dots, is present in cells resembling endothelial and smooth muscle cells of a blood vessel; I) Diaphragm processed using the *dapB* negative control probe: no labeling (red) is apparent.

but its genetic proximity to canine circovirus isolate 214 (GenBank accession no. JQ821392) and the association of canine circoviruses in dogs with vasculitis and hemorrhagic enteritis (Anderson et al., 2017; Decaro et al., 2014; Li et al., 2013) suggests a potential impact of BWCV on the health of susceptible cetaceans, which will require further research to define. Circoviruses are known to infect lymphoid tissues (Maclachlan and Dubovi, 2010). The BWCV labeling appeared subjectively greatest in cells morphologically resembling mononuclear immune cells, i.e. macrophages and lymphocytes, most notably in lymph nodes but also involving macrophages and lymphocytes in other tissues. The future development of immunohistochemical markers would assist in confirming our reported observation of a tropism of the BWCV for the mononuclear immune cells of the Longman's beaked whale. Using conventional ISH to PiCV, Smyth et al. (2001) found that cells positive for *Pigeon circovirus* (PiCV) were present both in cortex and medulla of lymphoid follicles and in interfollicular tissue of the bursa of Fabricius, and intense staining occurred mainly in cytoplasm of macrophages. In the liver, PiCV staining was commonly found in cells lining the sinusoids, thought to be Kupffer cells. Nonetheless, positive cells were also found within lymphoid aggregates and within discrete clusters of degenerate hepatocytes (Smythe et al., 2001). In the heart, lung, and tracheas, ISH-positive cells were located mainly in the interstitium, but occasional positive cells were seen in the epithelium of the trachea and airways in the lung (Smythe et al., 2001). In a study done by Rosell et al. (1999), PCV2 labeling were detected in cells of the monocyte/macrophage lineage including antigen-presenting cells, and lymphocytes, as well as epithelial cells, such as renal tubular cells, bronchial and bronchiolar cells, endothelial cells, and hepatocytes.

Additional techniques, such as transmission electron microscopy and quantitative PCR, could elucidate and correlate the intense staining of mononuclear immune cells with visual evidence of virus or viral load. The cerebrum and cerebellum tested positive for BWCV by conventional PCR but were not tested by ISH since these FFPE tissue blocks were not available. In the remaining nine tissues that tested positive for BWCV by conventional PCR, ISH confirmed the presence of BWCV nucleic acid in cells that were located in those PCR-positive tissues, with the exception of two that failed quality assessment of tissue nucleic acid (i.e. skeletal muscle and spleen). Taking into consideration that all the tissues tested were positive by PCR, systemic infection by this circovirus is thought to have occurred, which is further supported by the results of ISH. BWCV could be an opportunistic agent replicating in lymphoid tissues without clinical significance, or it may have contributed to disease in concert with the beaked whale morbillivirus and alphaherpesvirus previously reported in this stranded Longman's beaked whale juvenile (West et al., 2013).

The BWCV is the first circovirus to be detected in a cetacean, expanding the known host range of circoviruses to marine mammals, and we propose the formal species designation of beaked whale circovirus to be considered for approval by the International Committee on Taxonomy of Viruses. The role of the BWCV in the stranding of the juvenile Longman's beaked whale could not be determined in this study, and future research will be needed to define the role of this and

potentially other circoviruses in cetacean disease. Hawaii is home for many resident marine mammal populations including some that are critically endangered. Further research to investigate the prevalence and health impacts of circoviruses in marine mammals in Hawaii is warranted.

## CRediT authorship contribution statement

**Nelmarie Landrau-Giovannetti:** Writing - original draft, Writing - review & editing, Investigation, Formal analysis, Resources, Data curation. **Kuttichantran Subramaniam:** Writing - original draft, Writing - review & editing, Investigation, Formal analysis, Software. **Melissa Ann Brown:** Investigation, Writing - review & editing. **Terry Fei Fan Ng:** Investigation, Writing - review & editing. **David S. Rotstein:** Investigation, Writing - review & editing. **Kristi West:** Writing - review & editing, Conceptualization, Project administration, Funding acquisition, Resources, Data curation. **Salvatore Frasca:** Writing - original draft, Writing - review & editing, Investigation, Conceptualization. **Thomas B. Waltzek:** Writing - original draft, Writing - review & editing, Conceptualization, Investigation, Supervision, Project administration, Funding acquisition.

## Acknowledgments

We would like to thank the Hawaii marine mammal stranding response network volunteers for their participation in cetacean stranding responses throughout the main Hawaiian Islands. We are especially grateful to Nicole Davis who led the effort to recover the stranded Longman's beaked whale from Hana, Maui. We would also like to thank the NOAA John H. Prescott grant program for support of stranding response and diagnostics and the University of Florida for fellowship support to NLG who conducted this work as part her dissertation requirements.

## References

Abadie, J., Nguyen, F., Groizeleau, C., Amenna, N., Fernandez, B., Guereaud, C., et al., 2001. Pigeon circovirus infection: pathological observations and suggested pathogenesis. Avian Pathol. 30 (2), 149–158.

Anderson, C.M., Zhang, B., Miller, M., Butko, E., Wu, X., Laver, T., et al., 2016. Fully automated RNAscope in situ hybridization assays for formalin-fixed paraffin-embedded cells and tissues. J. Cell. Biochem. 117 (10), 2201–2208.

Biagini, P., Bendinelli, M., Hino, S., Kakkola, L., Mankertz, A., Niel, C., et al., 2012. Family *circoviridae*. In: King, A., Adams, M.J., Carstens, E.B., Lefkowitz, E.J. (Eds.), Virus Taxonomy: Classification and Nomenclature of Viruses: Ninth Report of the International Committee on Taxonomy of Viruses. Academic Press, London, pp. 343–349.

Breitbart, M., Delwart, E., Rosario, K., Segalés, J., Varsani, A., ICTV Report Consortium, 2017. ICTV virus taxonomy: circoviridae. J. Gen. Virol. 98 (8), 1997–1998.

Choi, C., Chae, C., 1999. In-situ hybridization for the detection of porcine circovirus in pigs with postweaning multisystemic wasting syndrome. J. Comp. Pathol. 121 (3), 265–270.

Decaro, N., Martella, V., Desario, C., Lanave, G., Circella, E., Cavalli, A., et al., 2014. Genomic characterization of a circovirus associated with fatal hemorrhagic enteritis in dog, Italy. PLoS One 9 (8), e105909.

Herbst, W., Willems, H., 2017. Detection of virus particles resembling circovirus and porcine circovirus 2a (PCV2a) sequences in feces of dogs. Res. Vet. Sci. 115, 51–53.

Ilyina, T.V., Koonin, E.V., 1992. Conserved sequence motifs in the initiator proteins for rolling circle DNA replication encoded by diverse replicons from eubacteria, eucaryotes and archaebacteria. Nucleic Acids Res. 20 (13), 3279–3285.

Katoh, K., Standley, D.M., 2013. MAFFT multiple sequence alignment software version 7: improvements in performance and usability. Mol. Biol. Evol. 30 (4), 772–780.

Kearse, M.G., Wilusz, J.E., 2017. Non-AUG translation: a new start for protein synthesis in eukaryotes. Genes Dev. 31 (17), 1717–1731.

Kedkovid, R., Woonwong, Y., Arunorat, J., Sirisereewan, C., Sangpratum, N., Lumyai, M., et al., 2018. Porcine circovirus type 3 (PCV3) infection in grower pigs from a Thai farm suffering from porcine respiratory disease complex (PRDC). Vet. Microbiol. 215, 71–76.

Kim, S.H., Park, J.Y., Jung, J.Y., Kim, H.Y., Park, Y.R., Lee, K.K., et al., 2018. Detection and genetic characterization of porcine circovirus 3 from aborted fetuses and pigs with respiratory disease in Korea. J. Vet. Sci. 19 (5), 721–724.

Kwon, T., Yoo, S.J., Park, C.K., Lyoo, Y.S., 2017. Prevalence of novel porcine circovirus 3 in Korean pig populations. Vet. Microbiol. 207, 178–180.

Firth, A.E., Brierley, I., 2012. Non-canonical translation in RNA viruses. J. Gen. Virol. 93 (7), 1385–1409.

Li, L., Kapoor, A., Slikas, B., Bamidele, O.S., Wang, C., Shaukat, S., et al., 2010. Multiple diverse circoviruses infect farm animals and are commonly found in human and chimpanzee feces. J. Virol. 84 (4), 1674–1682.

Li, L., Mcgraw, S., Zhu, K., Leutenegger, C.M., Marks, S.L., Kubiski, S., et al., 2013. Circovirus in tissues of dogs with vasculitis and hemorrhage. Emerging Infect. Dis. 19 (4), 534–541.

Lorincz, M., Csagola, A., Farkas, S.L., Szekely, C., Tuboly, T., 2011. First detection and analysis of a fish circovirus. J. Gen. Virol. 92 (8), 1817–1821.

Lorincz, M., Dán, Á, Láng, M., Csaba, G., Tóth, ÁG., Székely, C., et al., 2012. Novel circovirus in European catfish (*Silurus glanis*). Arch. Virol. 157 (6), 1173–1176.

Maclachlan, N.J., Dubovi, E.J., 2010. Circoviridae and anelloviridae. Fenner's Veterinary Virology, 4th ed. Academic Press, London, UK, pp. 259–268.

Mankertz, A., Hattermann, K., Ehlers, B., Soike, D., 2000. Cloning and sequencing of columbid circovirus (CoCV), a new circovirus from pigeons. Arch. Virol. 145 (12), 2469–2479.

Muhire, B.M., Varsani, A., Martin, D.P., 2014. SDT: a virus classification tool based on pairwise sequence alignment and identity calculation. PLoS One 9 (9).

Nayar, G.P., Hamel, A., Lin, L., 1997. Detection and characterization of porcine circovirus associated with postweaning multisystemic wasting syndrome in pigs. Can. Vet. J. 38 (6), 385.

Nguyen, L., Schmidt, H.A., Haeseler, A.V., Minh, B.Q., 2014. IQ-TREE: a fast and effective stochastic algorithm for estimating maximum-likelihood phylogenies. Mol. Biol. Evol. 32 (1), 268–274.

Palinski, R., Piñeyro, P., Shang, P., Yuan, F., Guo, R., Fang, Y., et al., 2017. A novel porcine circovirus distantly related to known circoviruses is associated with porcine dermatitis and nephropathy syndrome and reproductive failure. J. Virol. 91 (1), e01879–16.

Phan, T.G., Giannitti, F., Rossow, S., Marthaler, D., Knutson, T.P., Li, L., et al., 2016. Detection of a novel circovirus PCV3 in pigs with cardiac and multi-systemic inflammation. Virol. J. 13 (1), 184.

Phenix, K.V., Weston, J.H., Ypelaar, I., Lavazza, A., Smyth, J.A., Todd, D., et al., 2001. Nucleotide sequence analysis of a novel circovirus of canaries and its relationship to other members of the genus *Circovirus* of the family *Circoviridae*. J. Gen. Virol. 82 (11), 2805–2809.

Rambaut, A., 2014. FigTree v1. 2.2. Institute of Evolutionary Biology. University of Edinburgh.

Rosario, K., Breitbart, M., Harrach, B., Segalés, J., Delwart, E., Biagini, P., Varsani, A., 2017. Revisiting the taxonomy of the family *Circoviridae*: establishment of the genus *Cyclovirus* and removal of the genus *Gyrovirus*. Arch. Virol. 162 (5), 1447–1463.

Rosell, C., Segalés, J., Plana-Duran, J., Balasch, M., Rodrıguez-Arrioja, G.M., Kennedy, S., et al., 1999. Pathological, immunohistochemical, and in-situ hybridization studies of natural cases of postweaning multisystemic wasting syndrome (PMWS) in pigs. J. Comp. Pathol. 120 (1), 59–78.

Rozen, S., Skaletsky, H., 2000. Primer3 on the WWW for general users and for biologist programmers. Bioinform. Methods Protocols 365–386.

Sarker, S., Terrón, M.C., Khandokar, Y., Aragao, D., Hardy, J.M., Radjainia, M., et al., 2016. Structural insights into the assembly and regulation of distinct viral capsid complexes. Nat. Commun. 7, 13014.

Segalés, J., 2012. Porcine circovirus type 2 (PCV2) infections: clinical signs, pathology and laboratory diagnosis. Virus Res. 164 (1-2), 10–19.

Segalés, J., Kekarainen, T., Cortey, M., 2013. The natural history of porcine circovirus type 2: from an inoffensive virus to a devastating swine disease? Vet. Microbiol. 165 (1-2), 13–20.

Shibahara, T., Sato, K., Ishikawa, Y., Kadota, K., 2000. Porcine circovirus induces B lymphocyte depletion in pigs with wasting disease syndrome. J. Vet. Med. Sci. 62 (11), 1125–1131.

Smyth, J.A., Weston, J., Moffett, D.A., Todd, D., 2001. Detection of circovirus infection in pigeons by in situ hybridization using cloned DNA probes. J. Vet. Diagn. Investig. 13 (6), 475–482.

Stewart, M.E., Perry, R., Raidal, S.R., 2006. Identification of a novel circovirus in Australian ravens (*Corvus coronoides*) with feather disease. Avian Pathol. 35 (02), 86–92.

Tischer, I., Rasch, R., Tochtermann, G., 1974. Characterization of papovavirus and picornavirus-like particles in permanent pig kidney cell lines. Zentralbl. Bakteriol. Orig. A 226, 153–167.

Todd, D., Scott, A.N.J., Fringuelli, E., Shivraprasad, H.L., Gavier-Widen, D., Smyth, J.A., 2007. Molecular characterization of novel circoviruses from finch and gull. Avian Pathol. 36 (1), 75–81.

Todd, D., Weston, J.H., Soike, D., Smyth, J.A., 2001. Genome sequence determinations and analyses of novel circoviruses from goose and pigeon. Virology 286 (2), 354–362.

Wang, F., Flanagan, J., Su, N., Wang, L.C., Bui, S., Nielson, A., et al., 2012. RNAscope: a novel in situ RNA analysis platform for formalin-fixed, paraffin-embedded tissues. J. Mol. Diagn. 14 (1), 22–29.

West, K.L., Sanchez, S., Rotstein, D., Robertson, K.M., Dennison, S., Levine, G., et al., 2013. A Longman's beaked whale (*Indopacetus pacificus*) strands in Maui, Hawaii, with first case of morbillivirus in the central Pacific. Mar. Mamm. Sci. 29 (4), 767–776.